Rock Mech. Rock Engng. (2008) 41 (2), 343–371
DOI 10.1007/s00603-006-0099-2
Printed in The Netherlands

Rock Mechanics and Rock Engineering

Hydromechanical Behaviour of Rock-Bentonite Interfaces Under Compression

By

O. Buzzi[1], **M. Boulon**[1], **F. Deleruyelle**[2], and **F. Besnus**[2]

[1] Laboratoire Sols, Solides, Structures, Université Joseph Fourier, Grenoble, France
[2] Institut de Radioprotection et Sûreté Nucléaire, Fontenay aux roses, France

Received August 1, 2005; accepted March 8, 2006
Published online September 11, 2006

Summary

Interfaces between geomaterials may be critical for the long term confinement of the engineered barriers of nuclear waste disposals, particularly if there is water flow. Hydromechanical compression tests have been performed on rock-bentonite interfaces representing the contact between a host rock (toarcian argillite) and an engineered barrier within a nuclear waste repository. The results show that there is no major influence of the bentonite fraction or the nature of the additive as long as the additive is inert (sand or crushed rock): all the interfaces are closed for low values of normal stress (about 4 MPa). On the other hand, the hydromechanical behaviour of the interfaces changes when a high fraction of cement is used. Moreover, it has been shown that bentonite is very sensitive to hydraulic erosion, producing flow channels within the interface zone. A numerical study confirms the importance of erosion for the hydromechanical behaviour of the interface.

Keywords: Bentonite, rock, interface, hydromechanical, erosion, engineered barrier.

1. Introduction

In many countries (Canada, France, Sweden, Spain, Japan and others), the design of nuclear waste repositories is based on natural and engineered barriers to achieve long term confinement. Some Underground Research Laboratories (URL) have been developed to study the feasibility of such concepts. The materials involved (rock, concrete and bentonite mixtures) are now quite well known, but only limited information is available on the behaviour of contacts between these materials. However, it has been observed during a Tunnel Sealing Experiment (Dixon et al., 2002) that flow takes place within the contact between the host rock and the engineered barrier and not through the mass of these two elements when applying a pressure in the sealed chamber. The fact that interfaces may be critical zones for an engineered barrier has thus been emphasized.

Different kinds of contacts may affect a nuclear waste repository: rock joints, concrete-rock contacts, which are quite similar to rock joints (Kodikara et al., 1994; Seidel and Haberfield, 2002; Buzzi, 2004) and, bentonite-rock contacts. Some studies have been conducted on rock-bentonite interfaces in order to examine the hydration process of the buffer (Gens et al., 2002) or to investigate the evolution of the voids between the buffer and the rock due to bentonite swelling (Grindrod et al., 1999; Pusch, 1983; Marcial et al., 2001). Some shear tests on rock-bentonite are mentioned in the literature (Borgesson et al., 1996; Marcial et al., 2001) without displaying all the details and the results. Regarding the hydromechanical behaviour of such interfaces, almost no data are available. Not even in the study by Missana et al. (2003), dealing with water flow in a rock bentonite interface, is there any information about the hydraulic conductivity. Consequently, there is no quantification of the water flow through the interfaces. Yet, this is very significant information regarding the efficiency of the engineered barrier.

This paper deals with a study of the different possible mixtures that have been proposed in the literature as backfill material in the nuclear waste context. Pure bentonite has been rarely proposed for the engineered barrier, usually some materials (e.g. sand or crushed rock) are added to the bentonite in order to enhance its mechanical properties.

Bentonite-sand mixtures with half mass content of bentonite have been widely studied (Dixon et al., 1985, 2002; Tang et al., 2002; Tang and Graham, 2002; Graham et al., 2001) but, other mixtures are also used for the same purpose. The sand can be used at different mass fractions, ranging from 10 to 90%, (Santucci de Magistris et al., 1998; Chapuis, 2002; Al Shayea, 2001; Chijimatsu et al., 2000) and crushed rock can be used as an additive (Borgesson et al., 2003; Mata et al., 2001). In case of other kinds of waste for which the confinement is also crucial, some bentonite cement mixtures are sometimes employed (Koch, 2002; Garvin and Hayles, 1999). These authors have shown the influence of the mixture composition on its mechanical properties and hydraulic conductivity.

A possible in situ scenario of evolution of the rock-bentonite contact is progressive compression due to a combination of rock creep and of bentonite swelling. Once an equilibrium between these mechanism is reached, the voids between the natural and the engineered barriers should be filled and the waste should be properly confined. However, before reaching the equilibrium a transient phase is expected, during which geological water may flow in the interface subjected to a progressive compression.

The aim of this study is to identify the global qualitative behaviour of such interfaces subjected to compression. As for any contact, the transmissivity is expected to decrease when applying a normal stress, but the rock-bentonite interface requires a series of hydromechanical tests to fully describe its behaviour and the phenomena driving it. Another objective is to determine if one specific mixture should be used from the hydromechanical point of view. The experimental investigations are complemented by a hydromechanical uncoupled numerical study focused on the flow. Using a fluid mechanics software rather than expressing the transmissivity with the approximate cubic law enables us to calculate a number of relevant flow parameters useful for understanding the experimental results.

2. Experimental Facilities

2.1 Experimental Devices

The tests were performed using the direct shear box BCR3D and the associated hydraulic device. This apparatus has been designed by Boulon (1995) and developed by Armand (2000) and Hans (2002).

2.1.1 The Direct Shear Box BCR3D

This experimental device (Fig. 1) can be used for all classical interface compression and shear tests (constant normal stress, constant normal stiffness, constant volume) and has a shear velocity ranging from 0.05 mm/s to 50 cm/s through the use of both quasi static and dynamic electro-mechanical jacks. The BCR3D has been designed to avoid any relative rotation of the rock walls during the shear displacement. Such a relative rotation can greatly affect the quality of the tests (Boulon, 1995). Through the use of two actuators on the horizontal shear axis, the tangential relative displacement of both rock walls are symmetric with respect to the vertical (normal) axis, facilitating the application of the normal force on the joint. One advantage is that the normal force is kept centered on the surface of the joint thus preventing the upper part of the specimen from rotating. Each axis is equipped with one or two actuators (capacity of 100 KN) and with sensors measuring displacements and forces. Two LVDT's are

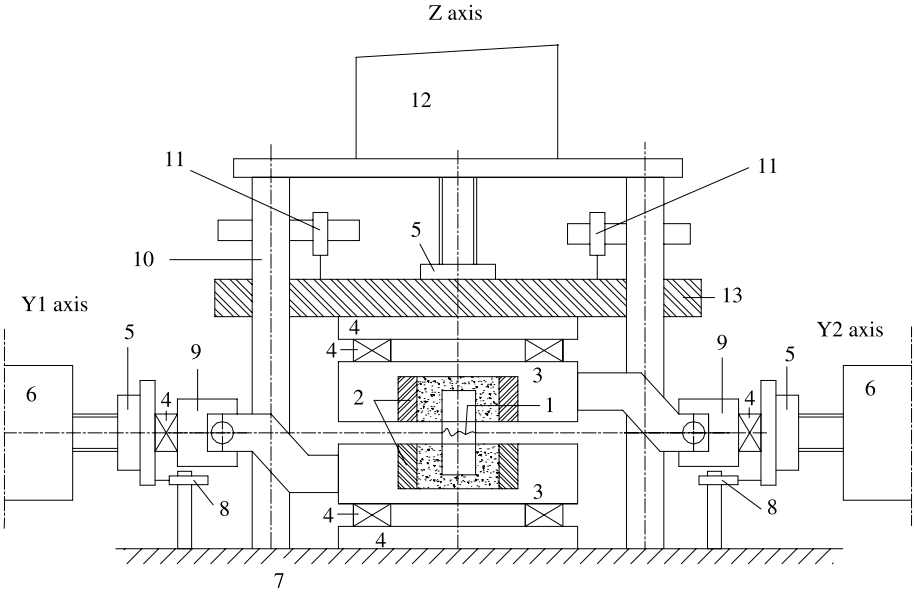

Fig. 1. Front view section along one shear axis of the BCR3D. *1*: interface specimen to be tested, *2*: internal removable metallic boxes, *3*: external boxes, *4*: sliding device enabling translation movements along axis X, *5*: load cells, *6*: horizontal actuators, *7*: rigid frame, *8*: displacement sensors (LVDT measuring Δy_1 and Δy_2), *9*: coupling device, *10*: rigid columns, *11*: displacement sensors (LVDT measuring Δz), *12*: vertical actuator, *13*: rigid vertically translating structure

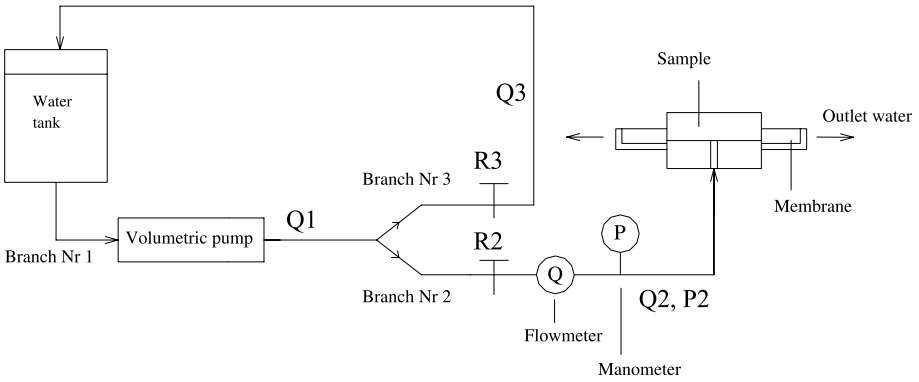

Fig. 2. Diagram of the hydraulic device. The pump injects a constant flow rate (*Q1*) into the circuit which is divided into two branches. One branch (*Nr3*) is the discharge whereas the other one (*Nr2*) goes to the specimen with a continuous measurement of flow rate and of pressure

used in the normal load axis to check that there is no parasite rotation during the shear test. A front view section of the apparatus is shown in Fig. 1. For this experimental program the BCR3D has been used only in compression.

2.1.2 The Associated Hydraulic Device

The diagram of the hydraulic device used for the hydromechanical tests is shown in Fig. 2. A constant water flow Q1 produced by the volumetric pump is injected into the hydraulic circuit which is divided in two branches: the first one (Nr3) is an adjustable discharge. The second branch (Nr2) is connected to the specimen with a continuous measurement of the pressure (P2) and the flow rate (Q2). Both hydraulic gates R2 and R3 are used to drive the test which is neither at constant injection pressure nor at constant flow rate. The outlet water (at atmospheric pressure) is collected by a membrane specially made for these tests in order to confine the bentonite.

2.1.3 The Membrane

Even when subjected to a 6 MPa compression, the bentonite is much less stiff than the rock. A high normal stress can thus not be applied on the interface specimen without confining the bentonite part. Moreover, the water flowing out of the interface has to be collected. The membrane is divided into five sectors in order to measure the flow in five directions and to be able to investigate the flow anisotropy. Either sectorial flows or total flow can be used depending on whether the anisotropy is studied or not. The membrane is made of an aluminium base for the mechanical boundary conditions and of a complementary elastomer part to have an efficient division into sectors and to prevent leakage during the test (see Fig. 3). Thus, the membrane places the bentonite in quasi oedometric conditions and enables water collection.

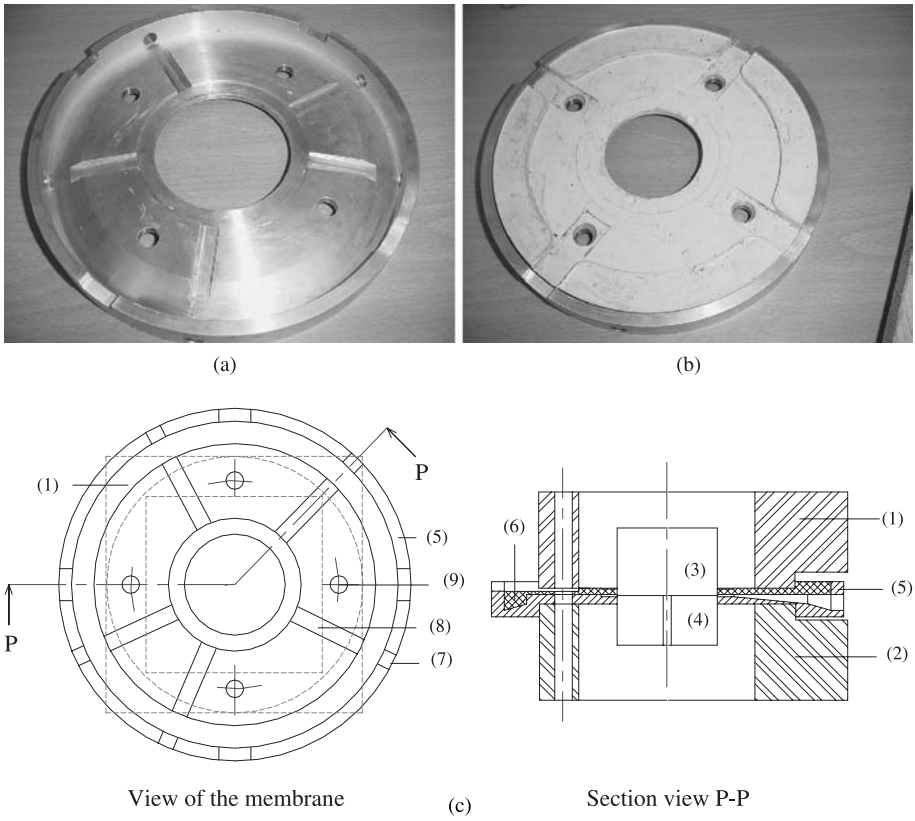

Fig. 3. Specific membrane designed for the rock-bentonite interfaces. **a**: Aluminium base of the membrane providing quasi oedometric boundary conditions. **b**: Complementary part in elastomer preventing leakage. **c**: Technical drawing of the membrane: plane view and section view. (*1*) and (*2*): metallic internal boxes (drawn in dots in the plane view). (*3*) and (*4*): Upper and lower parts of the specimen. (*5*): Aluminium part of the membrane. (*6*): Elastomer part of the membrane. (*7*) and (*8*): Channel and bore to collect the outlet water. (*9*): Bores for screws and metal guides used to assemble both parts of the specimen as shown on the section view and in Fig. 6

2.2 Experimental Program

Different bentonite mixtures have been tested to examine the influence of the bentonite fraction and the nature of the additive on the hydromechanical behaviour of the interface. The series of tests and the composition of the mixtures are given in Table 1.

All the tests are performed twice in order to verify their reproducibility and the relevance of the results. The first series of tests is shown in this paper while the complete set of results are available in Buzzi (2004).

2.2.1 Description of the Test

After installing the specimen in the experimental device, an initial normal stress of 0.3 MPa is applied (to avoid leakage). Thereby the water is forced to flow within the

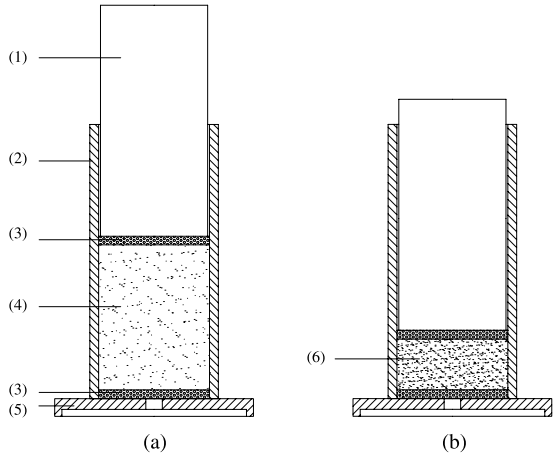

Fig. 4. Schematic representation of the compression of the bentonite mixtures. **a**: before compression: the bentonite mixture has a very high void ratio. **b** after the compression: the bentonite is compacted and the void ratio is lower. (*1*): piston, (*2*): cylindrical mold, (*3*): porous stones, (*4*): bentonite mixture before compression, (*5*): base, (*6*): compacted bentonite mixture

Table 1. List of the performed tests. The name of the test is defined by the bentonite mixture used. e.g. BS80: bentonite sand mixture with 80% in mass of bentonite. Each test is performed twice

Percent of bentonite in mass	Additives		
	Sand (S)	Crushed rock (R)	Cement (C)
50	BS50	BR50	1BC50
60	BS60	BR60	no test
70	BS70	BR70	no test
80	BS80	BR80	no test
90	BS90	BR90	1BC90

interface opening gate R2 (see Fig. 2) while both injection pressure and flow rate are measured. Once the hydraulic steady state has been reached (both injection pressure and flow rate constant), the total normal stress is increased. The final normal stress reached depends on the specimen behaviour and on any technical problems (e.g. leakage).

The test is performed neither at constant flow rate nor at constant pressure. An initial value of flow rate is imposed and the bentonite specimen subjected to compression acts as a gate. The flow rate will progressively decrease while the injection pressure increases when the normal stress increases. However, if the flow rate is too small to be measured, the operator can increase it in order to continue the test and to get relevant data. The tests are performed during loading and unloading of the specimen. Although the membrane allows one to investigate the anisotropy of the flow, the results are expressed considering the total flow. Indeed, the water flows only in one channel (see Sections 2.4 and 3) making an anisotropy study irrelevant.

2.2.2 Calculation of the Hydraulic Transmissivity

As in the case of rock joints, the rock bentonite interfaces are networks of voids described as a porous medium of permeability k saturated by water and obeying Darcy's law. Transmissivity tests are performed on annular specimens of interfaces and the flow is created by applying an injection overpressure ΔP of fluid at the internal radius (r_i) of the specimen while the atmospheric pressure (equal to zero) is applied at the external radius (r_e). As in many other studies (Hans and Boulon, 2003; Esaki et al., 1999; Lee and Cho, 2002), the tests can be interpreted in terms of

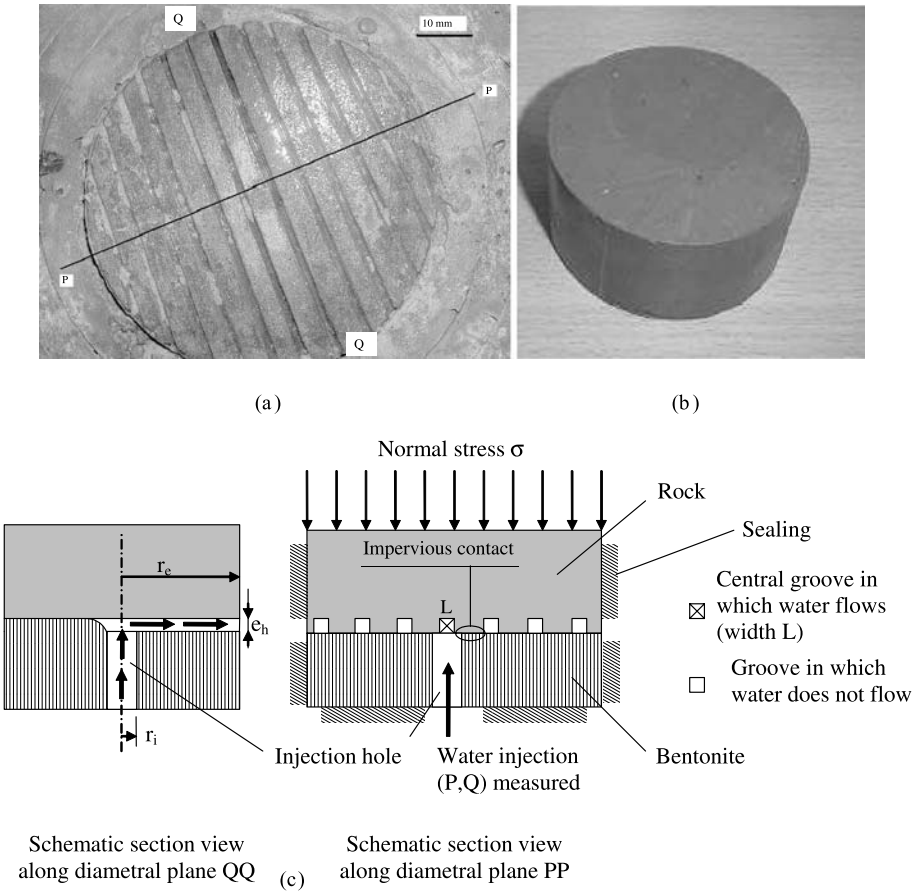

Fig. 5. Both parts of the interface specimen. **a** Rock specimen sealed in the metallic box with mortar. View of the hand made grooves (depth = 1mm, width = 1mm). **b** Bentonite part in which the central injection hole is not yet drilled (diameter 63 mm, height 30 mm). **c** Schematic section views along diametral planes (PP) and QQ (**a**) of the contact. The water is injected in the central hole with measurement of pressure (P) and flow rate (Q). Due to the alternance of groove and smooth impervious contacts, the water flows only in the central groove (marked with a cross). Due to the obstruction of one part of the central groove by the bentonite (left hand side of the groove), water flows only in one direction (towards the right hand side of the groove). Channel dimensions: L = 1 mm, $r_i = 2.5$ mm, $r_e = 31.5$ mm and e_h (average aperture). For the sake of clarity, normal stress and sealing are not shown on the section view along diametral plane QQ

isotropic transmissivity rather than in terms of permeability because this choice avoids making a hypothesis about the local hydraulic aperture.

The interfaces investigated in this paper are all made of a smooth bentonite wall, which can be subjected to important plastic strains, and of a stiff grooved rock wall. Then, assuming that the water flows in a channel (width L, length $(r_e - r_i)$ and average aperture e_h), as shown in Fig. 5(c), the intrinsic transmissivity T is expressed as:

$$T = \frac{(r_e - r_i)}{L} \cdot \mu \cdot \frac{Q}{\Delta P}, \tag{1}$$

with:

- T: intrinsic transmissivity [m^3],
- Q: flow rate [m^3/s],
- ΔP: internal injection pressure [Pa],
- r_e: external radius of the annular specimen [m],
- r_i: internal radius [m],
- L: width of the channel [m] (1 mm),
- μ: dynamic viscosity of the fluid [Pa.s] (1.005E-3 Pa.s at 20 °C).

The transmissivity t and the intrinsic transmissivity T are linked by $T = t \cdot \frac{\mu}{\gamma_w}$ with γ_w: volumic weight of the fluid [N/m^3]. The intrinsic transmissivity is used to express the results independently of the fluid properties. The temperature of the fluid, having an influence on its viscosity, has been measured during the whole test series and it varies significantly (from 16.5 to 25 °C). The changes of the physical properties of water with temperature is described in John and Haberman (1979). Using the table given in the appendix A, the viscosity of the fluid has been adjusted according to the temperature.

2.3 Materials

The rock used is an argillite of the Toarcian age from the IRSN experimental site of Tournemire. Many studies have been conducted on this material (Niandou et al., 1997; Daupley, 1997; Mathieu et al., 2000; Rejeb, 1999). This rock has a high clay fraction (70%) (kaolinite, illite, mectite, mica), from 10 to 20% calcite and from 10 to 20% quartz, it is saturated in its natural state and is highly anisotropic due to the bedding planes. Some mechanical data about the intact rock are available in Rejeb (1999). The Young's modulus ranges from 9 to 32 GPa depending on the location of the borehole. The water content is very low (from 1 to 5%) as is the hydraulic conductivity (from 10E-13 to 10E-15 m/s) after Rejeb (1999). This rock was also used for the bentonite-crushed rock mixtures as a rock dust ($D_{\max} \leq 2\,\mu m$) coming from the tunnel excavation phase.

The mineralogic composition of the natural Ca-bentonite used is given in Table 2. The Atterberg limits, determined in the laboratory, are $w_l = 120\%$ and $w_p = 190\%$, leading to a plasticity index I_p of 70%.

Table 2. Mineral composition of the bentonite FZ0

Minerals	Ca Montmorillonite	Illite	Kaolinite	Quartz	Calcite
Percentage	70 to 80	12 to 15	4 to 5	2 to 5	2 to 5

A silica sand has been used for preparing the bentonite-sand mixtures. The grain size ranges from 0 to 2.5 mm and the sand is characterized by a coefficient D85 = 1.7 mm (85% in mass of the particules have a diameter lower than D85) and a coefficient D10 = 180 μm. Finally, the cement used for the bentonite-cement mixtures is a standard cement CEM II/B 32.5R provided by Vicat company.

2.4 Specimen Preparation

As the argillite is very sensitive to hydration/dehydration (Charpentier et al., 2003), attention has been paid to the possible degradation of the rock within the interface zone during the test due to water and normal stress. To examine any modification of the rock, one rock specimen was used for each hydromechanical test rather than using replicas.

The bentonite mixtures have been prepared at the optimum water content (previous series of tests, (Buzzi, 2004) and have been left in plastic bags for a minimum of 48 hours to achieve a homogeneous water content. The mixture has then been subjected to a compression of 6 MPa (using the mold shown in Fig. 4) to get the bentonite part of the interface specimen (see Fig. 5b). This compression is not a consolidation of a saturated clay since the specimen is actually a kind of powder which is compressed during a few minutes. Under such conditions, the compression generates a drastic reduction of the void volume and a compaction of the clay but not expulsion of water. Due to the reduction of the void volume, the degree of saturation increases and at the end of the compression, the specimens are considered saturated. The same process has been followed for all specimens. The 5 mm diameter central injection hole is then drilled in the compacted bentonite specimen. Some parameters of the specimens are given in Table 3.

To highlight the influence of the mixture composition on the hydromechanical behaviour of the interfaces, the rock wall morphology must be constant. This is why we have chosen to create an artificial and reproducible roughness. Initially, the rock wall is smooth and the regular grooves are hand made with a saw before sealing the specimen to create the contact (see Figs. 5a and c).

A test, not shown in this paper but available in Buzzi (2004), has proven that an interface between smooth rock (without any grooves) and bentonite prevents water to flow even for high injection pressure. Due to the alternance of smooth contact and grooves and when the compression is applied, the water can only flow in the central groove since the water is prevented from flowing in any other direction. In theory, the flow should take place in the groove through the entire diameter of the specimen but it only occurred in one direction i.e. one radius. This can be explained by a difference in

Table 3. Saturation degree S, relative error on the saturation degree and dry volumetric weight γ_d of bentonite-crushed rock and bentonite-sand specimens

Mixtures	BS50	BS90	BR50	BR60	BR70	BR90
Saturation	1.002	1.006	1.01	1.005	1.08	1.02
Relative error $\Delta S/S$	0.09	0.05	0.07	0.06	0.24	0.06
$\gamma_d[kN/m^3]$	17	13	15.3	15.2	14.5	13.5

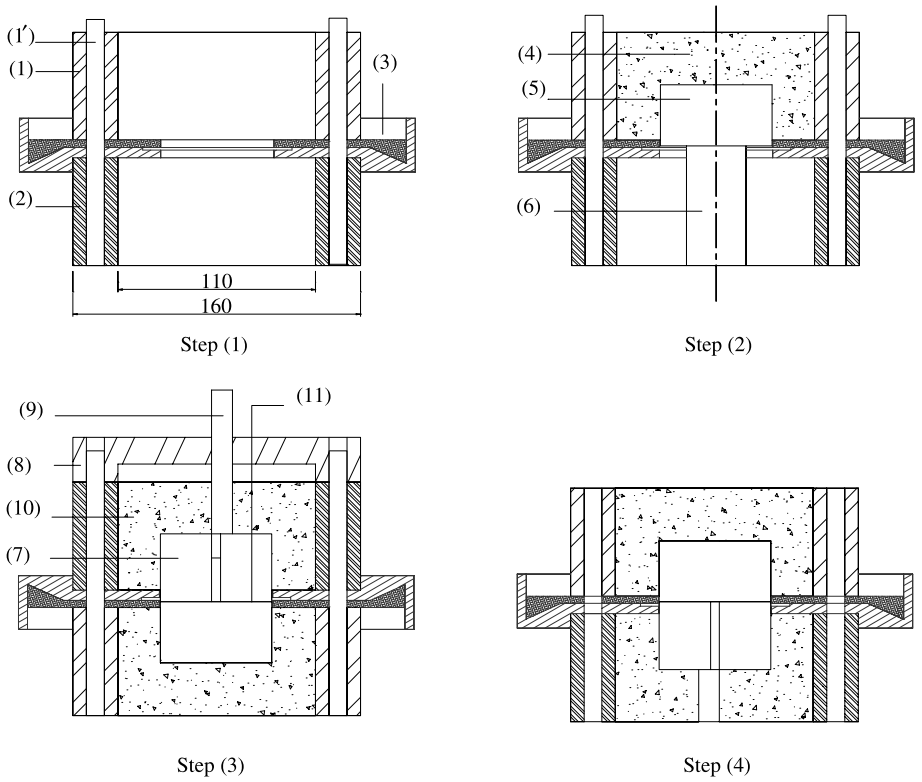

Fig. 6. Diagram of specimen preparation. Step 1: metallic boxes (*1*) and (*2*) and the membrane (*3*) are assembled using the pins (*1′*). Step 2: the rock specimen (*5*) is positioned using a wedge (*6*) and sealed with a mortar (*4*). Step 3: The bentonite part of the specimen (*7*) is placed on the rock part to create the contact (*11*). A steel cylinder with its support ((*8*) and (*9*) is positioned to create the injection hole in the mortar. Then, the mould is filled with mortar (*10*). Step 4: after a few hours, all pieces are removed and the interface specimen (*11*) can be tested

penetration of the bentonite into the groove and in its possible degradation by water between the two opposite radii. Figure 5c provides a schematic section view of the contact.

The steps of preparation of the interface specimen, designed for allowing radial flow, are explained in Fig. 6.

3. Experimental Results

The main goal of this experimental program is to investigate the hydromechanical behaviour of rock-bentonite interfaces. Figure 7 shows the evolution of the normal stress with respect to the normal relative displacement for test BR70. Due to the membrane, the normal stress has to be corrected to determine the real stress applied on the interface. This is done according to a procedure described in detail in Buzzi (2004). Three loading/unloading cycles have been performed on the specimen. They show a mechanical behaviour consistent with the mechanical boundary conditions

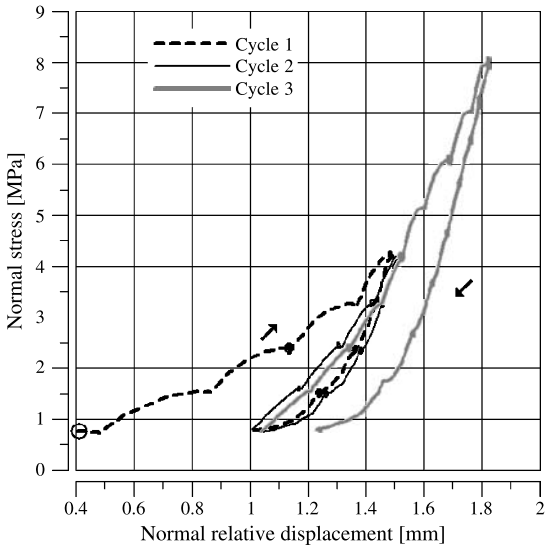

Fig. 7. Test BR70: evolution of the normal stress with respect to the normal relative displacement. Three cycles loading/unloading have been performed for this test. "O" represents the beginning of the test

(quasi oedometric compression) including a mechanical hysteresis and a stiffening of the material.

The load is increased step by step and after each load increment the hydraulic steady state is waited for, in order to register relevant values of pressure and flow rate.

Figure 8 shows the evolution of the intrinsic transmissivity with respect to the normal stress for the same specimen (BR70). The transmissivity decreases as the normal stress increases. The strained bentonite enters into the grooves of the rock, filling the voids and reducing the transmissivity. The large plastic strains of the bentonite lead to a closure of the interface under a low value of normal stress, between 3 and 5 MPa for all the tests. A transmissivity lower than $1E\text{-}16\,m^3$ means that the interface is closed. This value is very low in comparison to values related to rock joints (Hans and Boulon, 2003) or rock concrete interfaces (Buzzi, 2004) for which at least 10 MPa is required to obtain a contact closure.

Unloading the specimen (cycles 1 and 2) does not lead to an immediate opening of the interface. Indeed, the contact first remains closed due to the plastic strains of the bentonite still obstructing the grooves. It then opens progessively and the transmissivity increases. This is the reason that a hysteretic path can be seen of the transmissivity evolution. To investigate the hydromechanical behaviour of the interface for higher values of normal stress (greater than 2.6 MPa for cycle 3), it is necessary to enable the water to flow. To do so, the injection pressure is gradually increased by the operator until the interface is open and the water flows, thus increasing the transmissivity. Thereafter, the behaviour is the same as for previous cycles and the closure is still reached for higher values of normal stress (here 6 MPa and 8 MPa).

It has to be noticed that no modification of the rock, due to water flow, has been observed through the whole test series as it might perhaps have been expected. This

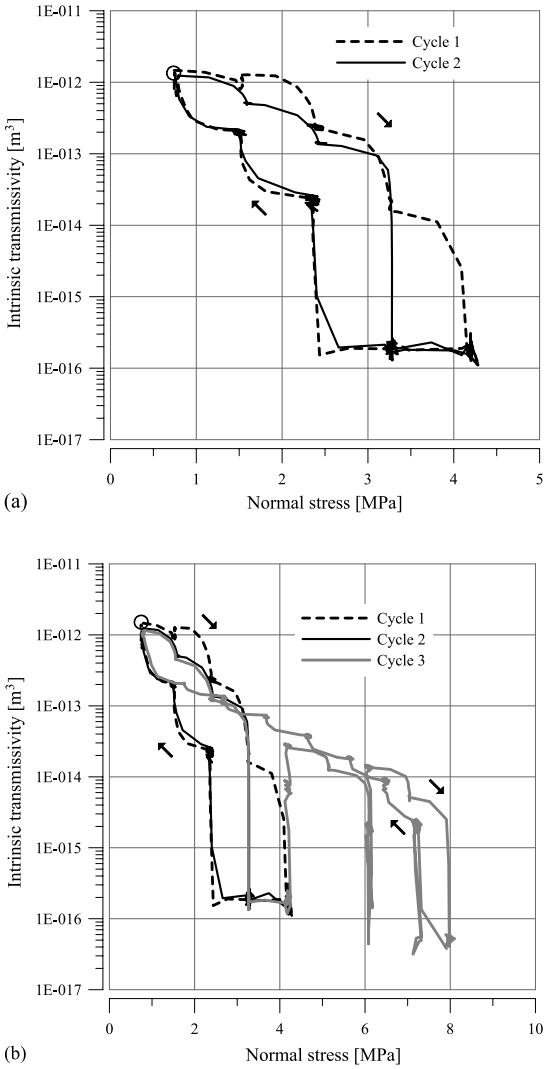

Fig. 8. Test BR70: evolution of intrinsic transmissivity with normal stress. **a** First two cycles, **b** All the cycles. "O" represents the beginning of the test. Maximum injection pressure: 1.7 MPa

could be explained by the average duration of the test, i.e. approximatively 3 hours, which is not long enough to affect the torcian argillite.

4. Discussion of the Experimental Results

The present study only involves hydromechanical coupling. The maximum duration of the test is 3 hours, the bentonite permeability and the injection pressure are very low (respectively about $1E\text{-}19\,m^2$ and lower than 0.5 MPa). We can therefore assume that there is no modification in the mass of the compacted bentonite (Pusch and Kasbhom,

2001), that there is no swelling during the test and that there is no chemical reaction since usual reaction times are greater than 3 hours (Di Maio, 2004).

4.1 Influence of the Bentonite Mixture

Another goal of this program is to determine if the mixture composition has an influence on the hydromechanical behaviour of the interface. Figures 9 and 10 show

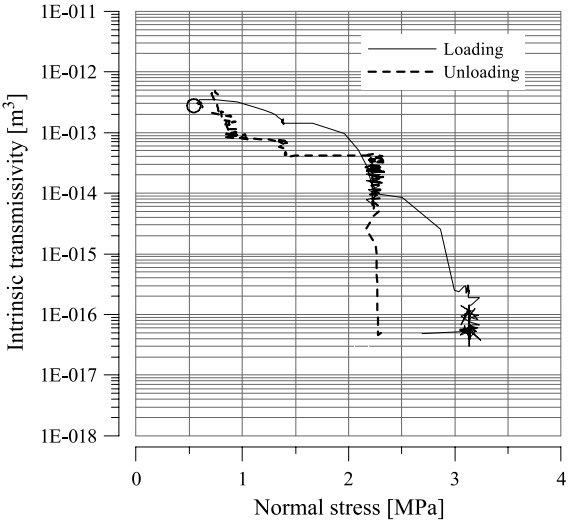

Fig. 9. Bentonite-sand mixtures: Test BS70. Evolution of intrinsic transmissivity with normal stress. O: beginning of the test. Maximum injection pressure: 2 MPa

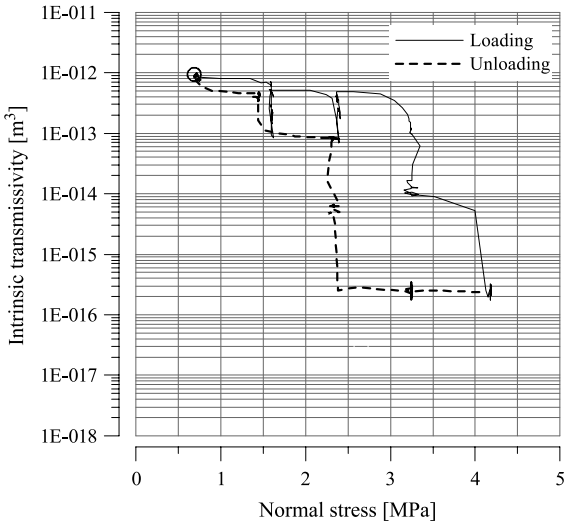

Fig. 10. Bentonite-crushed Rock mixtures: Test BR60. Evolution of intrinsic transmissivity with normal stress. O: beginning of the test. Maximum injection pressure: 0.4 MPa

the hydromechanical responses of typical mixtures made of inert additive (sand and crushed rock).

It is important to note that the initial transmissivity is very sensitive to the initial pressure and flow rate (Buzzi, 2004) and the initial measurement is thus not a relevant

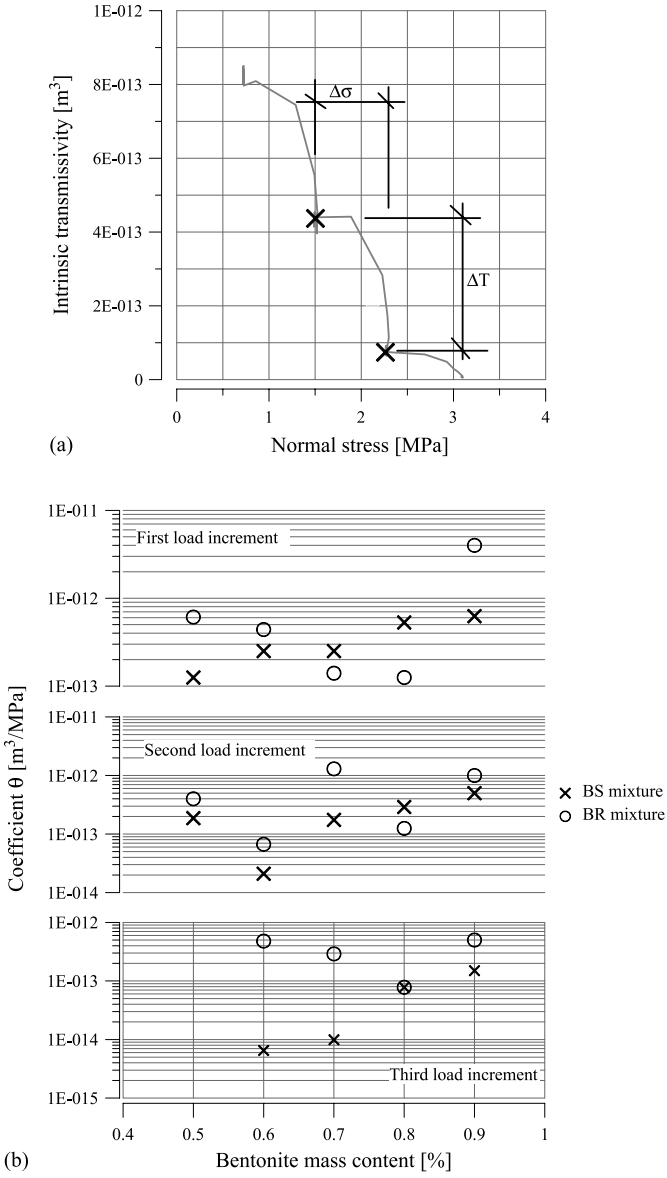

Fig. 11. Influence of the bentonite mixture. **a** Experimental evolution of transmssivity versus normal stress and definition of the coefficient θ for a load increment. θ is defined by: $\theta = \text{abs}(\Delta T/\Delta\sigma)$. **b** Evolution of θ versus bentonite mass content for bentonite sand and bentonite crushed rock mixtures and for the first three load increments

parameter to investigate the influence of the mixture. Actually, what can differ from one mixture to another and may be a reliable parameter, is the ability of the mixture to fill the voids and thereby close the interface to reduce the transmissivity. Therefore in order to better assess the responses of the different mixtures, a coefficient θ, defined by $\theta = abs(\Delta T/\Delta\sigma)$ for the three first load increments, is calculated (see Fig. 11a) to quantify the decrease of transmissivity as function of normal stress. Figure 11b shows the evolution of θ (for each load increment) with respect to the bentonite mass content. This figure proves that whatever the bentonite fraction or the additive used, all the hydromechanical responses are very close in terms of transmissivity decrease versus stress level.

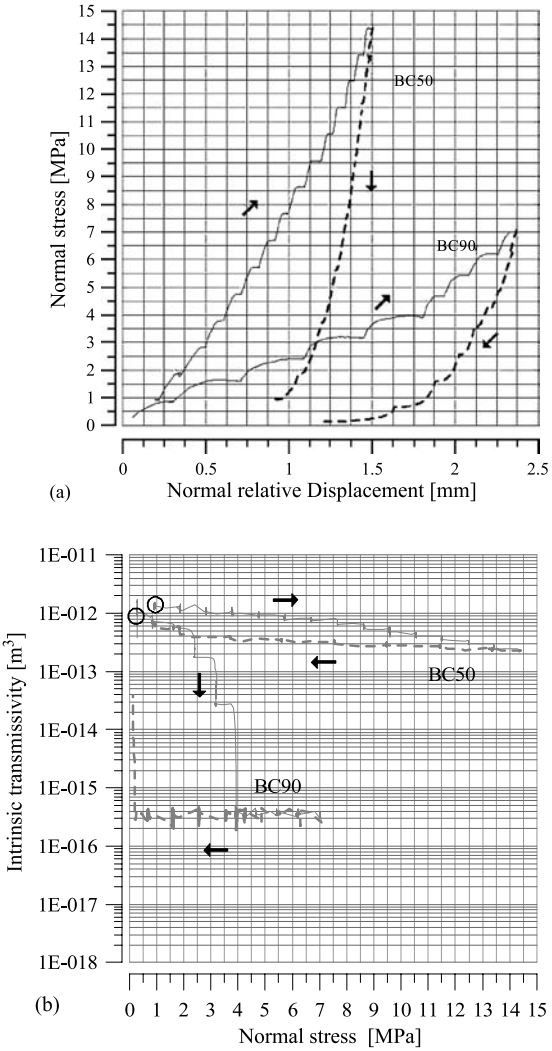

Fig. 12. Bentonite Cement mixtures: **a** Evolution of normal stress with normal relative displacement for tests BC50 and BC90. **b** Evolution of intrinsic transmissivity with normal stress for tests BC50 and BC90. O: beginning of the test

In some studies conducted on the mechanical or hydraulic behaviour of bentonite mixtures, it has been shown that the bentonite content can affect the mechanical or hydraulic properties of the mixture (Santucci de Magistris et al., 1998; Al Shayea, 2001; Chapuis, 2002; Borgesson et al., 2003). These results, which concern the material, can evidently not be extended to the interface. In the present study, no major influence of the mixture is found as regards the hydromechanical behaviour of the interface when the additive is inert (sand or crushed rock). As mentioned previously, the plastic strains of the bentonite can explain the hydromechanical behaviour of the rock-bentonite interface. The plastic behaviour of the bentonite is affected when adding cement. Indeed, the cement hydration generates brittle bonds in the material, turning the bentonite cement mixture into a quasi brittle material, even for low cement mass content (e.g. 10% of cement).

The first consequence is that the hydrated bentonite cement mixtures cannot be easily compacted since the application of large strains will break down the brittle bonds. The compaction must be undertaken as soon as possible after having mixed the water and dry mixture, otherwise the compacted bentonite blocks will crack and the density will not be as high as targeted, which can affect the efficiency of the engineered barrier.

Regarding the hydromechanical response, it appears in Fig. 12 that it is also affected by the cement content. The hydromechanical response of a low cement content mixture (BC90: 10% of cement) is very close to that of bentonite-sand or bentonite-crushed rock mixtures since the interface is closed for a value of normal stress equal to 4 MPa. On the other hand, for high cement content mixture (BC50: 50% of cement), higher values of normal stress, compared to bentonite-sand and bentonite-crushed rock mixtures, are required to close the interface. Actually, such a cement content highly affects the ductile behaviour of the bentonite and limits the plastic strains so that the response tends to be very similar to that of argillite mortar interfaces (Buzzi, 2004).

4.2 Degradation of the Bentonite by Water

All the bentonite parts of the interface specimens have been degraded by water during the tests, as shown in Fig. 13. If the test is stopped before reaching the interface closure, the bentonite is degraded as shown in Fig. 13a. This is due to the water flowing in the interface and it can be likened to erosion. This phenomenon can be detected by means of the evolution of the hydraulic parameters. Indeed, a sudden decrease of pressure and an increase of flow rate is generated, leading to an increase of transmissivity (Figs. 14a and b). Actually, bentonite is very sensitive to water. A flow against the bentonite surface generates a superficial modification of the bentonite into a gel like structure (Pusch, 1983; Grindrod et al., 1999).

Erosion can be explained by the shear stress applied by the flowing fluid on the soil (James et al., 1996; Pusch, 1983). However, there is no way to predict the erosion while performing the test since the key parameter is a local combination of pressure, flow rate and section of the flow (Buzzi, 2004).

When the interface is closed (no flow) and the pressure is strongly increased to resume the test (see Fig. 8), the interface is damaged as shown in Fig. 13b. This kind

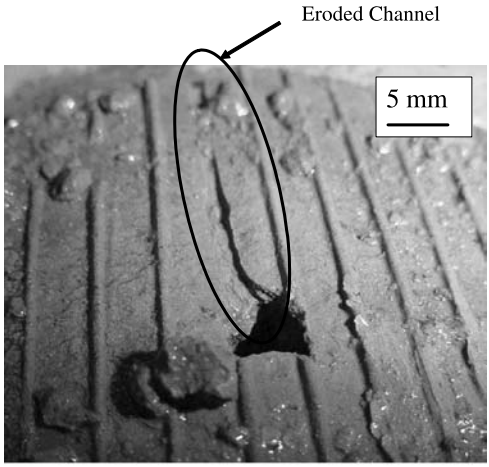

(a)

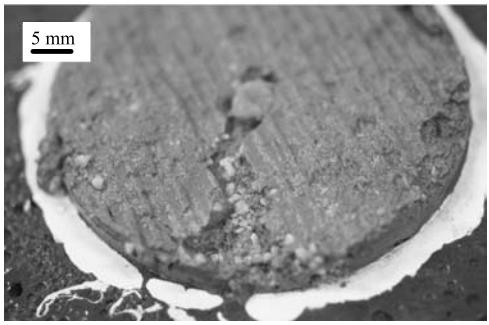

(b)

Fig. 13. Degradation of the bentonite part of the interface by the water: **a** Photograph of the eroded BR60 specimen. **b** Photograph of the eroded BS70 specimen

of degradation can be avoided by not increasing the injection pressure when the interface has been previously closed. For all the tests, the large strain supported by the bentonite leads to an interface closure for higher values of normal stress even with these two kinds of degradation (see Fig. 8).

4.3 Reproducibility of the Tests

The tests have been performed twice in order to check the relevance of the results. An identical response can hardly be obtained when testing twice the same mixture because each specimen is unique and very sensitive to water. Figure 15 shows the mechanical and hydromechanical responses for one bentonite cement mixture tested twice (mixture BC90, tests 1BC90 and 2BC90). The mechanical and hydromechanical curves are quite close before an erosion event damaging one contact. Afterwards, the hydromechanical responses are obviously different. In any case, Fig. 15 enables one to assess the reproducibility and the relevance of the results.

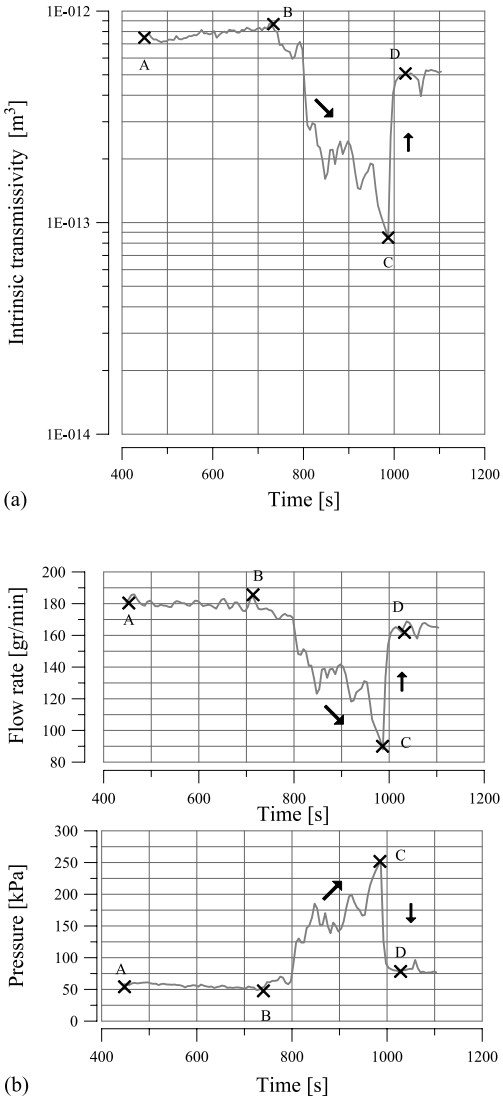

Fig. 14. Effects of erosion. Test BR60 (normal stress $\sigma = 1.6$ MPa). **a** Evolution of intrinsic transmissivity with respect to time. **b** Evolution of flow rate and pressure with respect to time. *A*: beginning of the test. *B*: an increment of normal stress is applied. Transmissivity and flow rate begin to decrease whereas pressure increases. *C*: erosion of the bentonite: transmissivity and flow rate suddenly increase whereas pressure decreases. *D*: erosion process has ended and the hydraulic parameters are stabilized

4.4 Flow Regime

One way to examine the flow regime (turbulent or laminar) is to increase or decrease pressure (resp. the flow rate) from an initial value and to investigate how flow rate (resp. pressure) evolves with respect to pressure (resp. flow rate). In the ''flow rate-pressure'' plane, a laminar flow is represented by a linear evolution of flow rate versus pressure (Jing and Stephansson, 1995; Zimmerman et al., 1998).

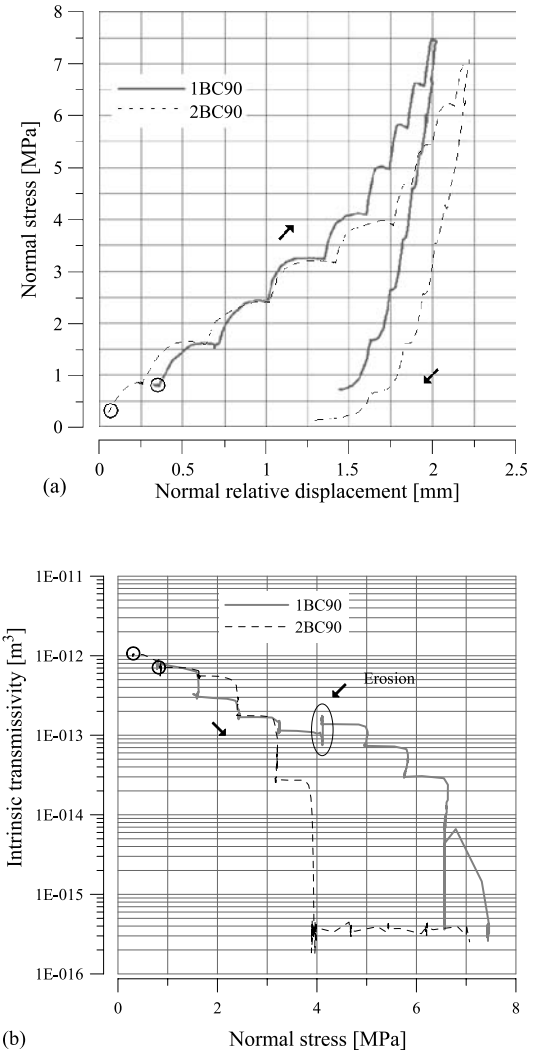

Fig. 15. Reproducibility of the results: bentonite cement mixture with 90% in mass of bentonite tested twice (Tests 1BC90 and 2BC90). **a** Mechanical response: evolution of normal stress versus normal relative displacement. **b** Hydromechanical response: evolution of transmissivity versus normal stress. An erosion event can be seen for test 1BC90. O: beginning of the test

Such investigations have been undertaken in this study and an example is shown in Fig. 16 for three differents levels of normal stress for test BR90 ($\sigma = 2.2$ MPa, 3.1 MPa and 4 MPa). Figure 16a shows the evolution of the flow rate and normal stress vesus time. The flow rate is successively decreased and increased for each normal stress and the corresponding evolution of flow rate versus pressure is reported in Fig. 16b. In this figure, the three cycles of decreasing/increasing the flow rate are visible: decreasing (resp. increasing) the flow rate leads to a decrease (resp. increase) of the pressure. It has to be noticed that the decrease of flow rate due to the augmentation of normal

stress (visible in Fig. 16a) corresponds, in Fig. 16b, to a drop of flow rate accompanied by an increase of pressure. In view of the evolution of flow rate with respect to pressure, the flow is assumed laminar for that test. However, other tests have shown that the flow is not always laminar, depending on the value of the flow rate and on the channel dimensions for each test. The numerical study presented below is also a way to assess the flow regime by means of the Reynolds number.

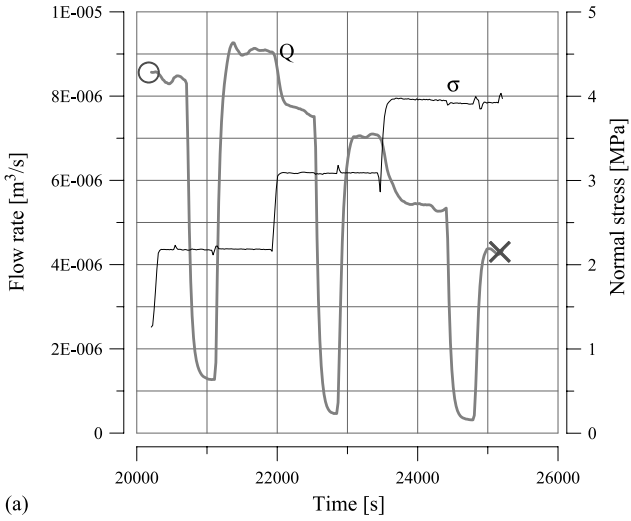

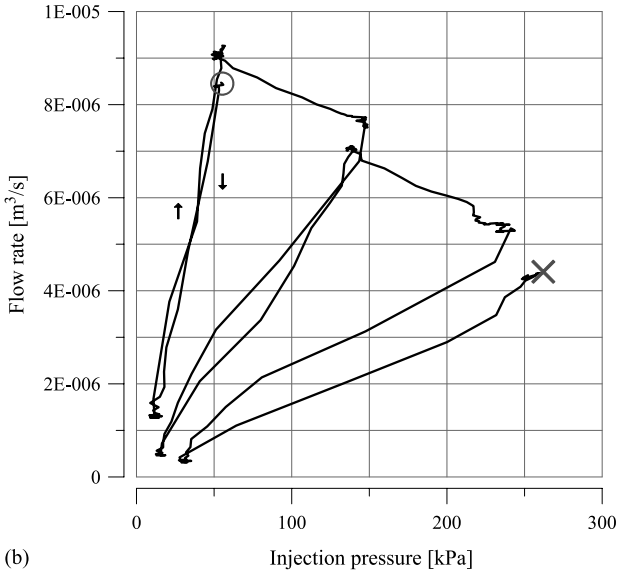

Fig. 16. **a** Evolution of normal stress σ and flow rate Q with respect to time for test BR90. **b** Evolution of flow rate versus pressure for the same test. O: beginning of the test. $\times$: end of the test

5. Numerical Study

This numerical part intends to study the flow within the interface using a fluid mechanics code (Fluent Inc., 1993) rather than expressing the transmissivity with the cubic law, so that the calculation of relevant flow parameters (e.g. Reynolds number, local velocity, shear stress, flow rate) is possible. To do this, an uncoupled numerical study is conducted by dividing the problem in two parts:

- The penetration of the bentonite into the rock grooves due to the compression is studied by a pure mechanical analysis using Abaqus (Hibbitt, Karlsson & Sorensen Inc., 1994) in order to obtain the void space in which the water flows.
- The obtained flow section is used to build a duct, in which the flow is simulated by pure hydraulic analysis using Fluent. The applied boundary conditions correspond to the experimental pressures (injection pressure at the inlet and atmospheric pressure at the outlet) and the transmissivity is calculated as for the hydromechanical tests.

5.1 Geometry and Mesh

The tests have shown that water flows into a central channel as shown in Fig. 5c, which constitutes the basic cell of the numerical study (see Fig. 17). The rock part is 2 mm high whereas the bentonite part is 42 mm in order to enable the bentonite penetration into the grooves. All the lateral displacements of the specimen are constrained. The problem is described using 3688 4-nodes elements built with 3954 nodes and the mesh is refined within the interface zone (see Fig. 17).

A Coulomb elasto plastic constitutive model has been used for both materials, the bentonite is described as a monophasic medium with the mechanical parameters (given in Table 4) being consistent with undrained parameters. Actually, the bentonite parameters are adjusted in order to get a numerical mechanical response as close as possible to the experimental one. Chosing ψ different from φ leads to a non-associated flow rule, which is desirable for geomaterials. Actually, the dilation angle ψ is taken as low as possible for reason of numerical convergence. A large strain calculation has been performed in view of the significant plastic strains observed during the tests.

The contact between both specimens is frictional ($f = 0.6$). A biphasic description of the bentonite including consolidation phenomena would have been more realistic, but this first approach focuses specifically on the flow and the mechanical part is only a necessary preliminary step to get some geometrical information.

Figure 18a shows the section resulting from the mechanical simulation, which is meshed for the Fluent calculation. This meshed section is extruded to build the duct shown in Fig. 18b and representing the channel made of bentonite and rock in which the water flows. The duct consists of 8-nodes hexaedral elements (from 160000 to 650000 elements according to the section) and the PRESTO and SIMPLEC algorithms of Fluent are used for the pressure and velocity coupling and calculation. In case of turbulent flow, the k–ε model developed by Launder and Spalding (1972) is used.

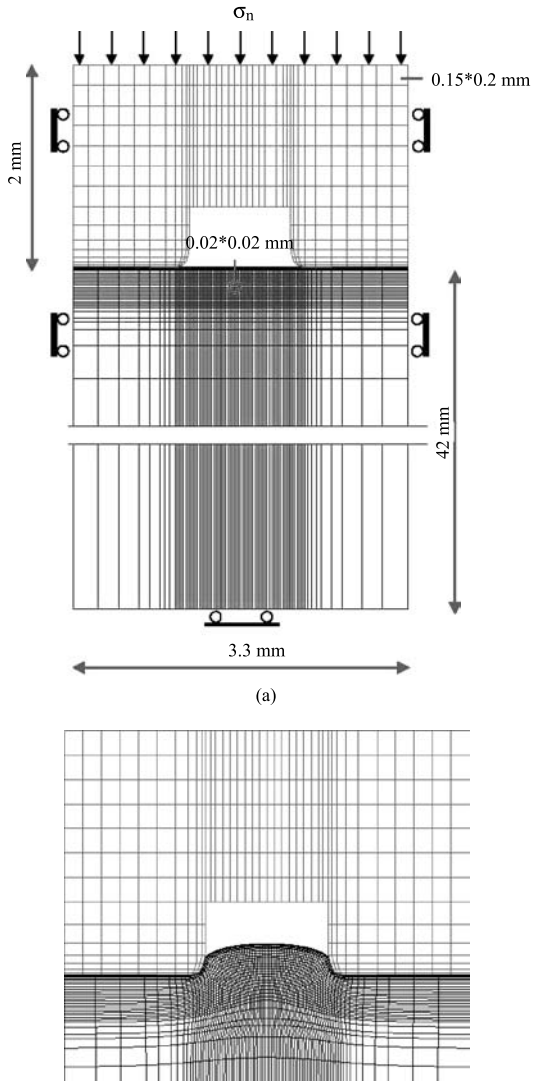

Fig. 17. Abaqus simulation: **a** Mesh geometry, dimensions and boundary conditions. **b** Penetration of the bentonite into the groove at $\sigma_n = 2$ MPa and view of the voids section used to simulate the duct for the hydraulic calculation

Table 4. Mechanical parameters of the bentonite and of the rock for the Abaqus calculation

	E [MPa]	c[kPa]	Dilation angle ψ [°]	Friction angle φ [°]	ν
Bentonite	22	120	16	24	0.45
Rock	2000	100	10	18	0.35

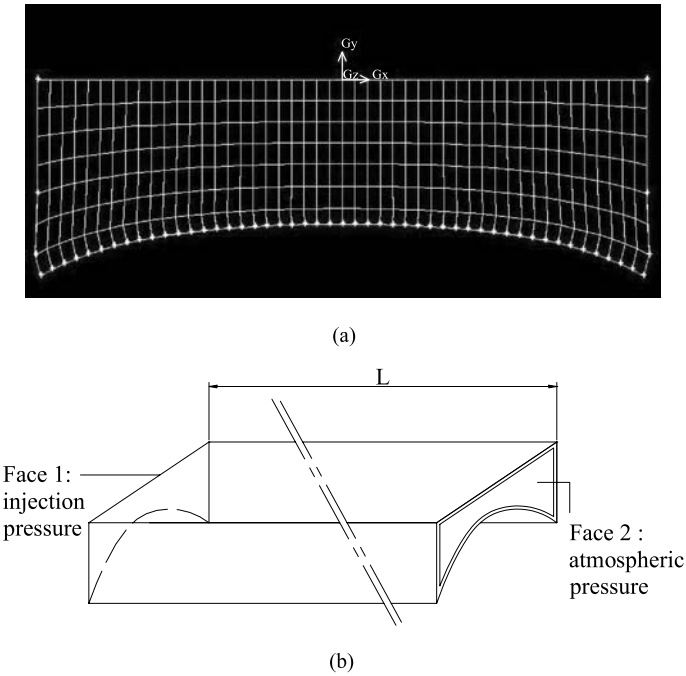

Fig. 18. "FLUENT" calculation. **a** View of the section coming from the mechanical simulation and meshed with Gambit. **b** View of the duct and of the boundary conditions. L = 29 mm

5.2 Numerical Results

The test BR60 has been used as a reference for this numerical study. For several values of normal stress, a duct has been formed on the basis of the mechanical calculation (see Fig. 19) and both experimental injection pressure and atmospheric pressure have been applied as boundary conditions. For each level of normal stress, the calculation has been performed according to a laminar or turbulent model depending on the Reynolds number which is expressed as $R_e = \frac{U \cdot D_h}{\nu}$ where:

- U is the average velocity [m/s],
- ν is the kinematic viscosity [m^2/s],
- $D_h = \frac{4 \cdot S}{P}$ with S the flow section [m^2/s] and P the hydraulic perimeter [m].

If R_e is lower than 2000 (resp. greater than 3000), the flow is considered to be laminar (resp. turbulent).

In case of R_e between 2000 and 3000, the flow regime can not be accurately defined (transition zone). Actually, the flow could be laminar or turbulent. Thus, both laminar and turbulent calculations are made. This explains the double value of the Reynolds number in Table 5. However, even with this double calculation, the flow regime can hardly be assessed. For test BR60, two erosion events occurred at $\sigma_n = 1.6$ and 2.4 MPa, leading to an important variation of pressure (decrease from $P = 250$ to 60 kPa and from $P = 280$ to 8 kPa). To see if it is possible to simulate the

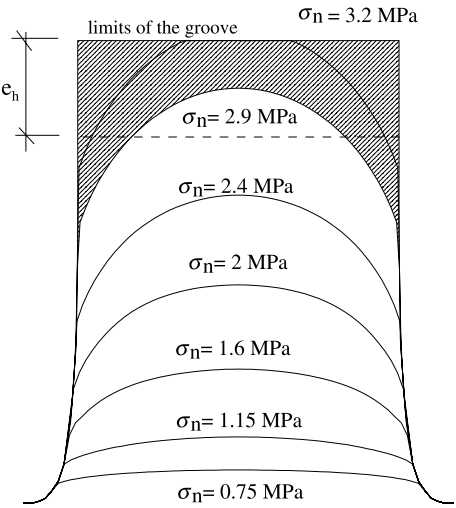

Fig. 19. Modeling of bentonite penetration profiles for different values of normal stress. Void section at $\sigma_n = 2.9$ MPa is represented in grey (mechanical calculation using "Abaqus"), e_h being the average aperture

Table 5. Hydraulic parameters used and calculated for the flow simulation

σ_n[MPa]	0.75	1.15	1.6		2	2.4		2.9	3.2
P_{exp}[kPa]	50	55	250	60	80	280	80	85	370
Q_{exp}[gr/min]	180	172	90	180	165	80	165	160	20
P_{num}[kPa]	54	52	240	*54*	*68*	*230*	77	83	380
				57	80	269			
Q_{num} [g/min]	141	140	263	*129*	*103*	*145*	54	8	7
					99	85	115		
Flow model	T	T	T	T and *L*	T and *L*	T and *L*	L	L	L
T_{num} [m^3]	1.2E-12	1.3E-12	5.3E-13	*1.1E-12*	*7.3E-13*	*3E-13*	3.4E-13	4.6E-14	8.9E-15
				8.4E-13	5.3E-13	2.1E-13			
R_e	3240	3300	6440	*3180*	*2560*	*3650*	1350	210	85
				2440	2200	2890			

σ_n: normal stress, P_{exp}: experimental injection pressure, Q_{exp}: experimental flow rate, P_{num}: numerical injection pressure, Q_{num}: numerical flow rate, T_{num}: numerical transmissivity, R_e: Reynolds number, L: laminar flow ($R_e < 2000$), *T*: turbulent flow ($R_e > 3000$), *T* and *L*: transition flow ($2000 \leq R_e \leq 3000$). In case of transition flow (*T* and *L*), two calculations have been performed: one laminar (*L*) and one turbulent (*T*). Italic results refer to laminar regime when both laminar and turbulent calculations are performed. At 1.6 MPa and 2.4 MPa, two calculations with different numerical injection pressures have been performed.

same variation of transmissivity just changing the boundary conditions, both values of pressure before and after erosion have been imposed. Then, two transmissivities have been calculated and confronted to the experimental results.

Table 5 summarizes the hydraulic parameters obtained by the Fluent calculation and the comparison between the experimental and the numerical evolution of the transmissivity with the normal stress is shown in Fig. 20.

The error on the numerical transmissivity can be estimated to be about 65% due to the uncertainty of the void section coming from the mechanical simulation. For the

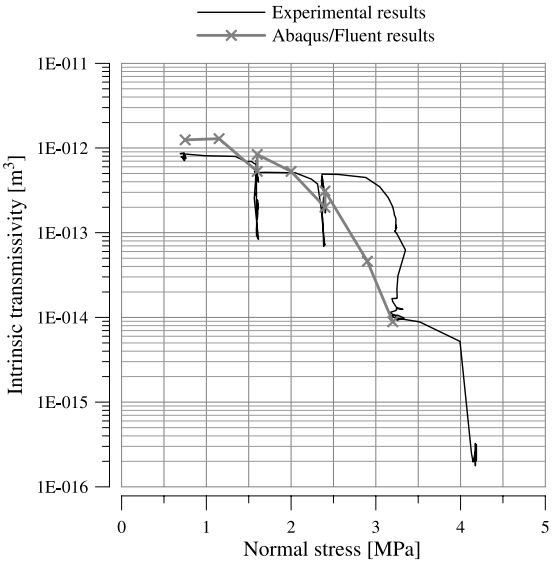

Fig. 20. Numerical and experimental evolution of the transmissivity with the normal stress. At 1.6 MPa, 2 MPa and 2.4 MPa, results of the calculation of the turbulent flow model are plotted

sake of clarity, no error bars are plotted in Fig. 20. This error is not that important considering the important experimental variations of transmissivity observed for a given value of normal stress. The numerical evolution of the transmissivity shown in Fig. 20 is very close to the experimental one.

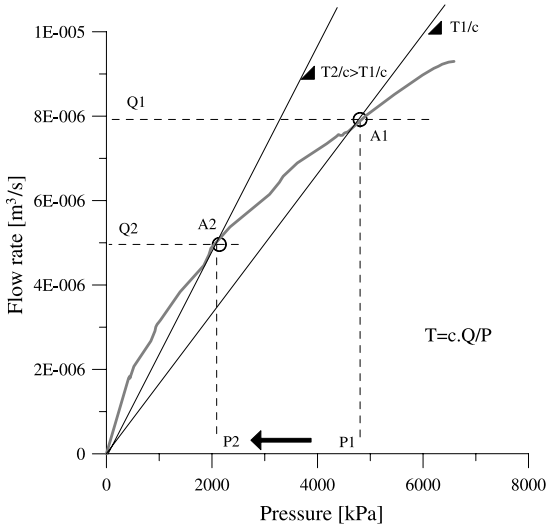

Fig. 21. Schematic evolution of flow rate versus injection pressure in an interface for a turbulent regime. The transmissivity is defined by $T = c \cdot Q/P$ with $c = \mu \cdot (r_e\text{-}r_i)/L$. The non linear evolution corresponds to a turbulent regime and leads to an increase of the transmissivity (from T1 to T2) when reducing the injection pressure (from P1 to P2)

It has been shown in Fig. 14 that erosion generates a decrease of pressure and an increase of flow rate, leading to an increase of transmissivity. Modifying the pressure conditions at the inlet of the duct from the pre-erosion pressure (e.g. $P = 250\,\text{kPa}$ at $\sigma_n = 1.6\,\text{MPa}$) to post-erosion pressure (e.g. $P = 60\,\text{kPa}$ at $\sigma_n = 1.6\,\text{MPa}$) leads also to an increase of transmissivity (see Fig. 20 at $\sigma_n = 1.6$ and $2.4\,\text{MPa}$). The Reynolds number calculation at both levels of normal stress show that the flow is within the transition zone between laminar and turbulent.

In the transition zone, the evolution of flow rate versus pressure becomes non linear (Jing and Stephansson, 1995) and a schematic evolution is shown in Fig. 21. This figure shows how dropping the pressure leads to an increase of transmissivity if the flow is turbulent. As a conclusion, the erosion effect (in terms of transmissivity augmentation) cannot be reproduced without modifying the interface as it occurs under erosion. Moreover, this simple simulation will inevitably lead to a closure of the interface whereas the real one can be opened by erosion.

The flow regime has been found to be laminar or turbulent at the different stages of the test and it appears that a low value of flow rate ($140\,\text{g/min}$ or $2.3\text{E-}6\,\text{m}^3/\text{s}$) can generate a turbulent flow ($R_e = 3300$). The flow has been found laminar for higher values of flow rate in Fig. 16b but the regime depends not only on the flow rate value but also on the flow section, which differs from one test to another.

6. Conclusions

The experimental and numerical study reported in this paper intends to investigate the hydromechanical behaviour of the rock-bentonite interfaces. In more classical contacts (e.g rock joints), the transmissivity is expected to decrease when applying normal stress. For rock-bentonite interfaces, the behaviour is not well known and required a series of hydromechanical tests to fully investigate the behaviour and the mechanisms driving it. Moreover, the influence of the mixture composition is often discussed regarding the mechanical properties or the permeability of the engineered barriers but, no data are available on its influence on the hydromechanical behaviour of the interface.

The tests have shown that, as for rock joints, the transmissivity decreases when the normal stress increases. The interfaces are closed for low values of normal stress (between 3 and 5 MPa). Whatever the mixture composition (when the additive is inert, such as sand or crushed rock), the interface closure is reached for the same range of normal stress. When the interface is closed and it is necessary to increase the injection pressure to force the water to flow, the bentonite part of the interface specimen is degraded (a channel is dug), which modifies the interface morphology and generates a large increase of transmissivity. It is important to notice that even in case of such a degradation, the interface closure can still be reached, thanks to the ductile behaviour of the bentonite mixtures.

The hydromechanical response of the contact can be highly affected by the use of cement (bentonite cement mixtures). The chemical reaction between cement and water prevents the bentonite cement mixture from having the same ductile properties as the bentonite sand or bentonite crushed rock mixtures. The first outcome is that the bentonite cement mixtures are difficult to compact. If hydration of cement starts before

compaction, then, the compacted bentonite blocks are likely to be cracked and less dense than targeted, affecting the efficiency of the engineered barrier. Furthermore, for high cement content mixtures (50% of cement in mass), the hydromechanical behaviour is very similar to that of rock joints due to a large increase of material stiffness.

As a conclusion, for an inert material (sand or crushed rock), there is no influence of its nature nor of the bentonite fraction (for contents of inert material ranging from 10 to 50% of the total mass of the mixture) on the hydromechanical behaviour of the interface. Similar to the findings of many authors, a superficial modification of the bentonite has been observed due to the water flow. The bentonite turns into a gel like structure, very sensitive to erosion, which can be seen as a shear stress threshold phenomenon. This erosion can not be accurately predicted.

The numerical study enabled us to quantify some local and global parameters of the flow (e.g. velocity, flow, pressure, shear stress). Thus, the transmissivity has been calculated using hydraulic parameters rather than using the basic cubic law. The flow regime can also be examined by means of the Reynolds number and it appears that even a low flow rate (140 gr/min) can generate a turbulent flow.

The numerical results are very close to the experimental ones but the variation of transmissivity due to erosion can not be properly reproduced. A consequence is that modeling the soil with a more sophisticated constitutive model is meaningless if the erosion is not taken into account.

References

Al Shayea, N. A. (2001): The combined effect of clay and moisture content on the behaviour of remolded unsaturated soils. Engng. Geol. 62, 319–342.

Armand, G. (2000): Contribution à la caractérisation en laboratoire et à la modélisation constitutive du comportement mécanique des joints rocheux. Thèse, Université Joseph Fourier, Grenoble, France.

Borgesson, L., Johannesson, L. E., Gunnarsson, D. (2003): Influence of soil structure heterogeneities on the behaviour of backfill materials based on mixtures of bentonite and crushed rock. Appl. Clay Sci. 23, 121–131.

Borgesson, L., Karnland, O., Johannesson, L. E. (1996): Modelling of the physical behaviour of clay barriers close to water saturation. Engng. Geol. 41, 127–144.

Boulon, M. (1995): A 3-d direct shear device for testing the mechanical behaviour and the hydraulic conductivity of rock joints. In: Proc., MJFR-2 Conference, Vienna, Austria, Balkema, Rotterdam, pp 407–413.

Buzzi, O. (2004): Hydromécanique du contact entre géomatériaux. Expérimentation et modélisation. Application au stockage de déchets nucléaires. Thèse, Université Joseph Fourier, Grenoble, France.

Chapuis, R. (1990): Sand bentonite liners: predicting permeability from laboratory tests. Can. Geotech. J. 27, 47–57

Chapuis, R. (2002): The 2000 r.m. hardy lecture: full scale hydraulic performance of soil bentonite and compacted clay liners. Can. Geotech. J. 39, 417–439.

Charpentier, D., Tessier, D., Cathelineau, M. (2003): Shale microstructure evolution due to tunnel excavation after 100 years and impact of tectonic paleo-fracturing. Case of Tournemire, France. Engng. Geol. 70, 55–69

Chijimatsu, M., Fujita, T., Kobayashi, A., Masashi, N. (2000): Experiment and validation of numerical simulation of coupled thermal, hydraulic and mechanical behaviour in engineered buffer materials. Int. J. Num. Anal. Meth. Geomech. 24, 403–424.

Daupley, X. (1997): Etude du potentiel de l'eau interstitielle d'une roche argileuse et de relations entre ses propriété hydriques et mécanique – application aux argilites du Toarcien de la région de Tournemire (Aveyron), Thèse – Ecole Nationale Supérieure des Mines de Paris.

Di Maio, C. (2004): Consolidation, swelling and swelling pressure induced by exposure of clay soils to fluids different from the pore fluid. Springer, Berlin Heidelberg New York pp. 19–43.

Dixon, D., Chandler, N., Graham, J., Gray, N. N. (2002): Two large scale sealing tests conducted at atomic energy of canada's underground research laboratory: the buffer-container experiment and isothermal test. Can. Geotech. J. 39, 503–518.

Dixon, D., Gray, M. N., Thomas, A. W. (1985): A study of the compaction properties of potential clay-sand buffer mixtures for use in nuclear fuel waste disposal. Engng. Geol. 21, 247–255.

Dixon, D. A., Martino, J. B., Chandler, A., Sugita, Y., Vignal, B. (2002): Water uptake by a clay bulkhead installed in the tunnel sealing experiment at atomic energy of Canada's underground research laboratory. In: Clays in natural and engineered barriers for radioactive waste confinement. Experiments in underground laboratories, Reims, ANDRA.

Esaki, T., Du, S., Mitani, Y., Ikusada, K., Jing, L. (1999): Development of shear-flow test apparatus and determination of coupled properties for a single rock joint. Int. J. Rock Mech. Min. Sci. 36, 641–650.

Garvin, L. S., Hayles, C. S. (1999): The chemical compatibility of cement-bentonite cut-off wall material. Constr. Build. Mater. 13, 329–341.

Gens, A., Guimaraes do N. L., Garcia-Molina, A., Alonso, E. E. (2002): Factors controlling rock-clay buffer interaction in a radioactive waste repository. Engng. Geol. 64, 297–308.

Graham, J., Yuen, K., Goh, T. B., Janzen, P., Sivakumar, V. (2001): Hydraulic conductivity and pore fluid chemistry in artificially weathered plastic clay. Engng. Geol. 60, 69–81.

Grindrod, P., Peletier, M., Takase, H. (1999): Mechanical interaction between swelling compacted clay and fractured rock, and the leaching of clay colloids. Engng. Geol. 54, 159–165.

Hans, J. (2002): Etude expérimentale et modélisation numérique multiéchelle du comportement hydromécanique de répliques de joints rocheux. Thèse, Université Joseph Fourier Grenoble.

Hans, J., Boulon, M. (2003): A new device for investigating the hydromecanical properties of rock joints. Int. J. Numer. Anal. Meth. Geomech. 27, 513–548.

Hibbitt, Karlsson & Sorensen Inc. (1994): Abaqus Theory Manual.

Fluent Inc. (1993): Fluent User's guide. Vol. 1, 2 and 3.

James, P. W., Jones, T. E. R., Stewart, D. M. (1996): Numerical and experimental studies of annular flume flow. Appl. Math. Modelling 20, 225–231.

Jing, L., Stephansson, O. (1995): Mechanics of rock joints: experimental aspects. In: Selvadurai, M. P. S., Boulon, M. J. (eds.) Mechanics of geomaterial interfaces. Asterdam, Elsevier, pp 317–342.

John, J. E. A., Haberman, W. L. (1979): Introduction to fluid mechanics, 2nd edn. Prentice Hall, Englewood Cliffs.

Koch, D. (2002): Bentonites as a basic material for techical base liners and site encapsulation cut off walls. Appl. Clay Sci. 21, 1–11.

Kodikara, J. K., Johnston, I. W. (1994): Shear behaviour of irregular triangular rock-concrete joints. Int. J. Rock Mech. Min. Sci. Geomech. Abstr. 31(4), 313–322.

Launder, B. E., Spalding, D. B. (1972): Mathematical models of turbulence. Academic Press, New York.

Lee, H. S., Cho, T. F. (2002): Hydraulic characteristics of rough fractures in linear flow under normal and shear load. Rock Mech. Rock Engng. 35(4), 299–318.

Marcial, D., Delage, P., Cui, Y. J. (2001): Reduced model test for the study of the self sealing capacity of the joints of bentonite based engineered barriers. In: 6th International Workshop on Key Issues in Wastes Isolation Research (KIWIR), pp 285–303.

Mata, C., Guimaraes, L., Ledesma, A., Gens, A., Olivella, S. (2001): A hydro geomechanical analysis of the saturation process with salt water of a bentonite crushed rock mixture in an engineered nuclear barrier. In: 6th International Workshop on Key Issues in Wastes Isolation Research (KIWIR), pp 643–663.

Mathieu, R., Pagel, M., Clauer, N., De Windt, L., Cabrera, J., Boisson, J. Y. (2000): Paleofluids circulations records in shale: a mineralogical and geochemical study of calcite veions from experimental Tournemire tunnel site (France).

Missana, T., Alonso, U., Turrero, M. J. (2003): Generation and stability of bentonite colloids at the bentonite/granite interface of a deep geological radioactive waste repository. J. Contam. Hydrol. 61, 17–31.

Niandou, H., Shao, J. F., Henry, J. P., Fourmaintraux, D. (1997): Laboratory investigations of the mechanical behaviour of the tournemire shale. Int. J. Rock. Mech. Min. Sci. 34(1), 3–16.

Pusch, R. (1983): Stability of bentonite gel in crystalline rock – physical aspects. Technical Report TR-83-04, SKB, Lund, Sweden.

Pusch, R., Kasbhom, J. (2001): Can the water content of highly compacted bentonite be increased by applying a high water pressure?, Technical Report TR-01-33, SKB, Lund, Sweden.

Rejeb, A. (1999): Mechanical characterisation of the argillaceous tournemire site (France). In: Site characterisation practice. IBH Publ., Oxford, pp 45–50.

Santucci de Magistris, F., Silvestri, F., Vinale, F. (1998): Physical and mechanical properties of a compacted silty sand with low bentonite fraction. Can. Geotech. J. 35, 909–925.

Seidel, J. P., Haberfield, C. M. (2002): A theoretical model for rock joints subjected to constant normal stiffness direct shear. Int. J. Rock Mech. Min. Sci. 39, 539–553.

Tang, G. X., Graham, J., Blatz, J., Gray, M., Rajapakse, R. K. N. D. (2002): Suctions, stresses and strengths in unsaturated sand-bentonite. Engng. Geol. 64, 147–156.

Tang, X. G., Graham, J. (2002): A possible elastic-plastic framework for unsaturated soils with high plasticity. Can. Geotech. J. 39, 894–907.

Zimmerman R. W., Yeo W. I., De Freitas M. H. (1998): Effect of shear displacement on the aperture and permeability of a rock fracture. Int. J. Rock Mech. Min. Sci. 35, 1051–1070.

Authors' address: Olivier Buzzi, Laboratoire Sols, Solides, Structures, Université Joseph Fourier, BP 53, 38041 Grenoble, Cedex 9, France; e-mail: olivier.buzzi@hmg.inpg.fr